

Observing Population Transfer in a Two-Photon Dressed Field Three-Level System by Transient Stimulated Emission

Huei Tarng Liou,^{*,†} Kuang Lang Huang, and B. Fain[‡]

Institute of Atomic and Molecular Sciences, Academia Sinica, P.O. Box 23-166, Taipei, Taiwan, and School of Chemistry, Tel-Aviv University, Ramat-Aviv, Israel

Received: March 24, 1997; In Final Form: July 11, 1997[⊗]

In a three-level CS₂ system coupled with two pulsed photon fields, we have observed stimulated emission at a time when the stimulating photon pulse precedes the pump photon pulse by 2.5 pulse widths. This counterintuitive time sequence in photon–matter interaction was interpreted by a model as emission resulting from photon dressed transient states (superposition of molecular quantum states in a Schrödinger equation approach) evolution. The model calculation is also able to simulate the observed quantum interference between two populated levels.

I. Introduction

Photon fields in a multiphoton event may interact incoherently or coherently with matter (CS₂ molecules in the present work). The former can usually be described by a rate equation approach. To establish rate equations, certain populations occupying defined molecular states are essential. The states involved in this incoherent process are the molecular quantum states characterized by electronic, vibrational, and rotational states. In this rate equation approach, the sequence of population transfer between states follows the pulse sequence of photon fields. However, this is not always true when the molecular quantum states are dressed by strong photon fields. Oreg et al.,¹ Gaubatz et al.,² and Schiemann et al.³ have applied a so-called STIRAP technique (stimulated Raman adiabatic passage) to experimentally demonstrate a counterintuitive interaction sequence of two photon fields. Using this technique, they achieved an efficient (>95%) state-selected population transfer between a thermally populated vibrational level and a highly excited vibrational level of the ground electronic state of (Na)₂ and NO. These two levels are coupled to a common level of an upper excited state by a pump photon and a Stoke photon. The thermally populated level and the upper level are coupled by the pump photon while the highly excited vibrational level and the upper levels are coupled by the Stoke photon. Population transfer between the thermally populated level and the highly excited vibrational level was cut short by applying the counterintuitive sequence of the two photon fields. It is called “counterintuitive” because the interaction begins with the Stoke photon and is followed by the pump photon. STIRAP greatly improved the efficiency of population transfer, so Gaubatz et al.⁴ suggested that complete population transfer could be reached. It implies that one shall not observe any emission from the upper molecular quantum state where no population has actually accumulated in the process. In fact, this is only true under the circumstances that the laser fields have zero line width and in addition the time difference between two laser fields apparently needs to be optimized. On the other hand, the efficiency could also be influenced by dark resonances.⁵ Emission, therefore, becomes an indication for the efficiency

of population transfer. We have monitored the stimulated emission in a pump-stimulating pulse system to investigate the efficiency of population transfer varying with the time difference between the pump and the stimulating photons. Preliminary results in the previous work⁶ showed a connection between efficient population transfer and the counterintuitive order of the applied laser pulses. Those results were partially explained by an approximate adiabatic solution to a three-level Schrödinger equation. We have extended Khidekel et al.’s⁶ work, by taking the detuning of laser frequency and the laser line width into account. The Hamiltonian including the detuning term is solved explicitly. The resulting numerical calculations successfully simulate the emission profile from experimental observations. Both the counterintuitive sequence and the quantum interference of the observed emissions are explained by the dressed photon approach.

II. Experiment

A three-level system subjected to two pulsed laser fields is depicted in Figure 1. $|1\rangle$ represents $J = 30, (0\ 0\ 0), X^1\Sigma_g^+$; $|2\rangle$ represents $J = 31, (0\ 10\ 0), R^3B_2$; and $|3\rangle$ represents $J = 32, (3\ 18\ 0), X^1\Sigma_g^+$. Detailed spectroscopic information on the above levels has been studied by many researchers. The actual spectroscopic data used in this work was taken as follows: for $J = 30, (0\ 0\ 0), X^1\Sigma_g^+$ from Wells et al.;⁷ for $J = 31, (0\ 10\ 0), R^3B_2$ from Merer et al.;⁸ and for $J = 32, (3\ 18\ 0), X^1\Sigma_g^+$ from Liou et al.⁹

The stimulated emission pumping (SEP) was carried out on CS₂. The experimental setup of SEP in a polarization spectroscopy scheme was described in previous papers.^{6,9} Briefly, two photon pulses generated by two dye lasers (Lambda Physik FL3002) were individually pumped by two excimer lasers (Lambda Physik Lp208 and Lp200 ic). The time delay between these two photon pulses was controlled by a digital pulse-delay generator (SRS DG535) with picosecond resolution. The pulse duration of the output of each laser is 25 ns, and the laser line width is 0.2 cm⁻¹. The pump photon pulse and the stimulating photon pulse propagated in opposite directions. (From now on in this paper, to avoid confusion we use s-active photon pulse to denote the stimulating photon pulse and s-passive photon pulse to denote the stimulated photon pulse). The pump photon pulse was circularly polarized, while the s-active photon pulse was linearly polarized. Two polarizers were placed across each

* Author to whom correspondence should be addressed. Fax number: 011 886 2 3620501. E-mail: htliou@po.iam.s.sinica.edu.tw.

[†] Academia Sinica.

[‡] Tel-Aviv University.

[⊗] Abstract published in *Advance ACS Abstracts*, December 1, 1997.

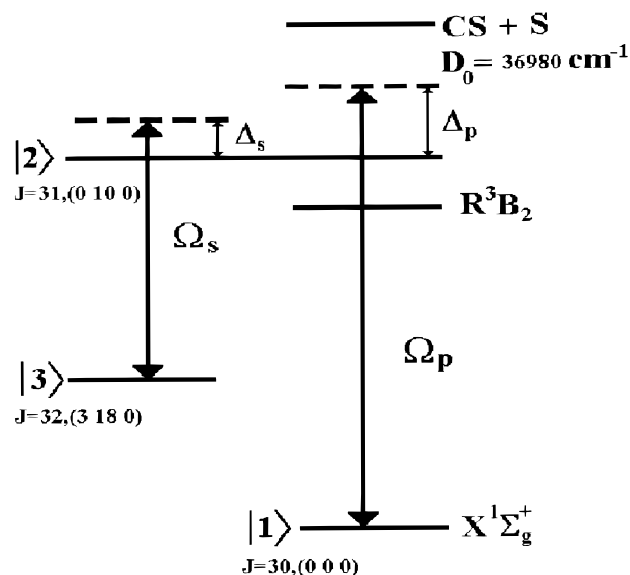


Figure 1. The energy level of SC_2 subjected to two laser fields. Ω_p is the pump pulse Rabi frequency wavelength at 343.2 nm; Ω_s is the stimulating pulse frequency wavelength at 507.2 nm. Δ_p and Δ_s are the detunings from the resonance frequencies of the system.

other at the entrance and the exit of the cell tube. The cell is a 135 cm long stainless steel tube and filled with 350 mTorr of CS_2 .

According to Teets et al.,^{10,11} for a linearly polarized excitation photon, the emission intensity I as function of detuning frequency x is expressed as

$$I = I_0 \left[\xi + \theta^2 + b^2 + \frac{1}{2} \theta \Delta \alpha L \frac{1}{1+x^2} + \frac{1}{2} b \Delta \alpha L \frac{x}{1+x^2} + \frac{1}{4} (\Delta \alpha L)^2 \frac{1}{1+x^2} \right] \quad (1)$$

where θ is the uncrossing angle, ξ is the finite transition at $\theta = 0$, b is the birefringence of the cell window, L is the length of cell, and $\Delta \alpha = \alpha^+ - \alpha^-$ is the difference in the absorption coefficients for the right- and left-hand circularly polarized s-active photon pulse components. Ideally, without the terms containing ξ , θ , and b , two polarizers (when crossed with each other) could totally block the s-active photon pulse but allow s-passive photon pulse to pass through the exit polarizer. This s-passive photon pulse was detected by a photodiode and was registered as the signal in the scheme of polarization spectroscopy.

III. Results and Discussion

To record stimulated emission vs delay time spectrum, the first step is to pretune the pump and the s-active photon pulses to the resonant frequencies. When the pump photon pulse was fixed at the exact resonance and the s-active photon pulse frequency was scanned, it was observed that the single-peaked feature of $|2\rangle$ to $|3\rangle$ transition gradually splits into a multi-peaked feature as the intensity of either the pump laser or the s-active laser is increased. A typical spectrum with two Lorentzian line shape peaks is shown in Figure 2. The separation between the split peaks increases with the intensity of the lasers. This indicated an Autler–Townes doublet effect,^{12,13} except that it was observed for a molecule. More complicated features (more than two peaks) were observed as the photon intensity was further increased. A double-peaked spectrum generally appeared for a strong pump and a weak s-active photon pulses.

Maximum emission shifted away from the exact resonance due to the splitting, as shown in Figure 2. This implies that

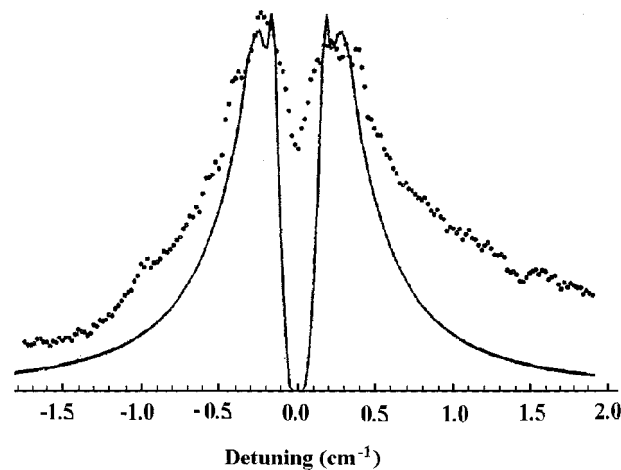


Figure 2. The stimulated emission vs detuning spectrum. The spectrum was recorded by scanning the frequency of the stimulating photon with intensity of 10 mJ, while the pump photon was fixed at the exact resonance with intensity of 12 mJ. The time delay between two photon fields is zero. Splitting and power broadening in the transition are observed. Points are experimental observations; while the solid curve is the simulation resulting from the dressed state approach.

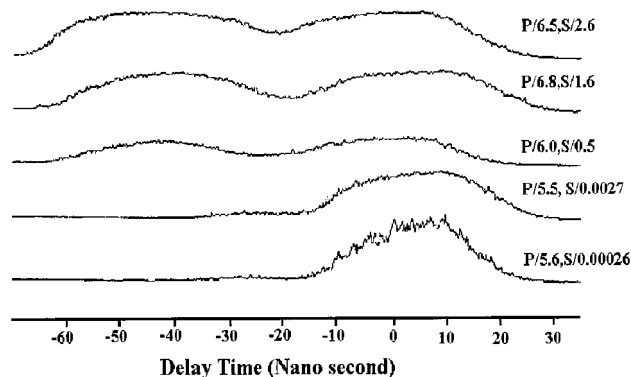


Figure 3. The stimulated emission vs delay time plot. Delay time is negative when the stimulating photon pulse precedes the pump photon pulse. The frequencies of the two lasers were fixed at the exact resonance. The intensities of lasers vary, but the pump laser is mostly kept constant. The pump laser of 6.5 mJ and the stimulating laser of 2.6 mJ, for instance, are denoted as P/6.5,S/2.6.

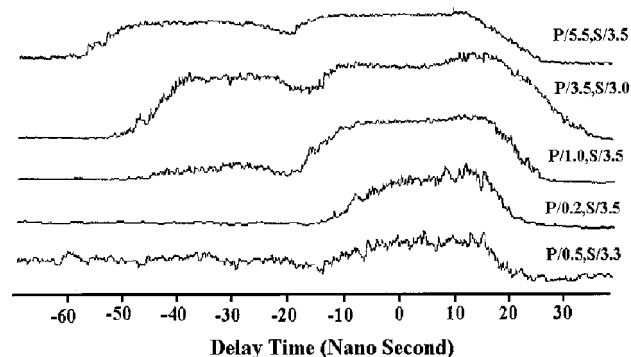


Figure 4. The stimulated emission vs delay time plot. Delay time is negative when the stimulating photon pulse precedes the pump photon pulse. The frequencies of the two lasers were fixed at the exact resonance. The intensities of lasers vary, but the stimulating laser is mostly kept constant. The pump laser of 5.5 mJ and the stimulating laser of 3.5 mJ, for instance, are denoted as P/5.5,S/3.6.

the efficiency of population transfer to the $|2\rangle$ state or $|3\rangle$ state can be manipulated by detuning the frequency of the s-active photon pulse. That is, to achieve maximum stimulated emission, one shall detune the s-active photon pulse from exact resonance. Also, emission not dropping to zero at the exact resonance

implies that complete population transfer to state $|3\rangle$, in addition to counterintuitive interaction sequence, can only be achieved provided that lasers possess no line width, no fluctuation in time. Time delay scans were taken by recording the intensity of stimulated emission at each delay time. This delay time is the arrival time difference between two laser pulses. Negative delay time means that the s-active photon pulse preceded the pump photon. The frequency of the pump photon pulse was fixed at the exact resonance, while the s-active photon pulse, based on the energy resolved spectrum such as Figure 2, was tuned to the frequency where maximum stimulated emission occurred. Time delay scans taken under various intensities of the pump laser and constant intensity of the s-active laser are shown in Figure 3.

Scans taken under various intensities of the s-active laser and constant intensity of the pump laser are shown in Figure 4.

The emission at negative delay gradually increases with the laser intensity, as indicated in both figures. The emission could even be observed at -60 ns delay time, more than 2.5 pulse durations of the laser, where two laser pulses are hardly overlapped. These observations cannot be regarded as a STIRAP experiment in which the adiabatic following condition has to be fulfilled. From the rate equation approach point of view, it requires specific molecular state to be occupied to initiate emission or absorption. Molecular states' properties confine $\langle 1|2\rangle = 0$, $\langle 2|3\rangle = 0$ at any time. Consequently, without interaction no emission can be observed unless molecular states interact with photon fields yielding $\langle 2|\Omega_p|1\rangle \neq 0$ to make $\langle 3|\Omega_s|2\rangle \neq 0$. At the delay time of -60 ns $\Omega_p = 0$, it is difficult to see how to build up the population in state $|2\rangle$, which is essential to stimulated emission. Thus, from population transfer point of view, one may regard Figures 3 and 4 as the experimental observations indicating a counterintuitive interaction sequence in the scheme of stimulated emission. However, viewing from the dressed state approach, the emission does not necessarily result from a stationary state that is prepared by interacting with photon field. "Counterintuitive sequence" may be described as a consequence of transient state evolution. In the dressed state expression the evolution is illustrated to be

$$|1,2,3,\Omega_s\rangle \rightarrow |1,2,3,\Omega_s,\Omega_p\rangle \rightarrow |1,2,3,\Omega_p\rangle$$

In the following, we derive the dressed state wave function and establish the density matrix. This density matrix can be phenomenologically probed by stimulated emission in the scheme of polarization spectroscopy during the evolution. We show that the results can be used to explain the observation.

A. Theoretical Consideration. Under the assumption that magnetic sublevel is degenerated,¹⁴⁻¹⁶ the Hamiltonian that describes the molecular J -level interacting with the two-photon field in a matrix form is expressed as

$$H = \frac{1}{2}\hbar \begin{pmatrix} -2\Delta_p & \Omega_p & 0 \\ \Omega_p & 0 & \Omega_s \\ 0 & \Omega_s & -2\Delta_s \end{pmatrix} \quad (2)$$

$$\Omega_p = \frac{\mu_{12}E_p(t)}{\hbar} \quad (3)$$

$$\Omega_s = \frac{\mu_{23}E_s(t)}{\hbar} \quad (4)$$

$$E_i(t) = \frac{1}{2}(E_i^0(t)e^{-i\omega_i t} + c.c.) \quad (5)$$

Ω_p is the pump pulse Rabi frequency; Ω_s is the s-active pulse frequency. Δ_p and Δ_s are the detunings from the resonance

frequencies of the system. $E_i(t)$ and ω_i represent the electric field and the frequency of the associated photon field, respectively.

First consider the case with $\Delta_p \neq 0$, but $\Delta_s = 0$. By defining

$$\sin \theta = \frac{\Omega_p}{(\Omega_p^2 + \Omega_s^2)^{1/2}} \quad (6.1)$$

$$\cos \theta = \frac{\Omega_s}{(\Omega_p^2 + \Omega_s^2)^{1/2}} \quad (6.2)$$

$$\tan \theta = \frac{(\Omega_p^2 + \Omega_s^2)^{1/2}}{(\Omega_p^2 + \Omega_s^2 + \Delta_p^2)^{1/2} - \Delta_p} \quad (6.3)$$

the eigenvectors can be expressed as²

$$|a^0\rangle = \cos \theta|1\rangle - \sin \theta|3\rangle \quad (7.1)$$

$$|a^+\rangle = \sin \phi \sin \theta|1\rangle + \cos \phi|2\rangle + \sin \phi \cos \theta|3\rangle \quad (7.2)$$

$$|a^-\rangle = \cos \phi \sin \theta|1\rangle - \sin \phi|2\rangle + \cos \phi \cos \theta|3\rangle \quad (7.3)$$

and the eigenvalues of $|a^\pm\rangle$ and $|a^0\rangle$ are

$$\omega^\pm = -\frac{1}{2}[\Delta_p \mp (\Delta_p^2 + \Omega_p^2 + \Omega_s^2)^{1/2}] \quad (8.1)$$

$$\omega^0 = -\Delta_p \quad (8.2)$$

The wave function, coupled to the radiation field, can be written as²

$$|\Psi(t)\rangle = \alpha^+ |a^+(t)\rangle + \alpha^0 |a^0(t)\rangle + \alpha^- |a^-(t)\rangle \quad (9.1)$$

In the adiabatic following condition,

$$|\Psi(t)\rangle \approx |a^0(t)\rangle \quad (9.2)$$

Experimentally this condition is ensured by

$$\sqrt{\Omega_p^2 + \Omega_s^2} T \gg \frac{\Delta t}{T} \quad (9.3)$$

where T is the half-width at half-maximum of the pulse duration and Δt is the time delay.

Interaction begins with the s-active photon pulse $\Omega_s \gg \Omega_p$ to make $\cos \theta \approx 1$ and $\sin \theta \approx 0$, leading to $|\langle 1|a^0\rangle| \approx 1$ at early time. Later, the arrival of the pump photon pulse toward to the end of the interaction $\Omega_p \gg \Omega_s$ to make $\sin \theta \approx 1$, leading to $|\langle a^0|3\rangle| \approx 1$. This implies that the population transfer from state $|1\rangle$ to state $|3\rangle$, provided that the evolution of the state vector $|\Psi(t)\rangle$ follows $|a^0\rangle$ adiabatically throughout the interaction. Consequently, no population is accumulated in state $|2\rangle$ in the above process. It implies that no stimulated emission shall be observed. However, this is the ideal case and is only true under the circumstances that spectral line widths are negligible. This can be understood more clearly from the plot of the population of state $|2\rangle$ vs the detuning given in Figure 2 of ref 17 as well as in Figure 2 of this work. The population of $|2\rangle$ state in ref 17 was represented by the fluorescence intensity, while in this work it is represented by stimulated emission. In the two figures the profiles of population $|2\rangle$ state show a double-peaked feature. The splitting between these two peaks can be described by a Lorentzian hole that centers at zero detuning. The full width at half-maximum of the hole is proportional to the square of the Rabi frequency of both the

pump and the probe photon fields. The splitting implies that a detuning, whose value depends on the strength of the applied fields, will be introduced once the molecular states are dressed by the interacting photon fields. Furthermore, because the system interacts with pulsed fields, this detuning shall also have profiles in time domain. Since the detuning is appreciable, as shown in Figure 2, Δ_s in eq 2 shall be considered non-zero.

Now we consider the case $\Delta_p = 0$, $\Delta_s \neq 0$. In the dressed state approach, by defining the following

$$S2 = \Delta_s^2 + 3\Omega_p^2 + 3\Omega_s^2 \quad (10.1)$$

$$S3 = 2\Delta_s^3 - 18\Delta_s\Omega_p^2 + 9\Delta_s\Omega_s^2 \quad (10.2)$$

$$S6 = -4\Delta_s^4\Omega_p^2 + 8\Delta_s^2\Omega_p^4 - 4\Omega_p^6 - 20\Delta_s^2\Omega_p^2\Omega_s^2 - 12\Omega_p^4\Omega_s^2 - \Delta_s^2\Omega_s^4 - 12\Omega_p^2\Omega_s^4 - 4\Omega_s^6 \quad (10.3)$$

$$Sh = (S3 + \sqrt{27(S6)})^{1/3} \quad (10.4)$$

the eigenvalues of Hamiltonian H in eq 2 can be expressed as

$$\omega_a = \frac{\Delta_s}{3} + \frac{Sh}{54^{1/3}} + \frac{2^{1/3}S2}{3Sh} \quad (11.1)$$

$$\omega_b = \frac{\Delta_s}{3} + \frac{i}{2}\sqrt{3}\left(\frac{Sh}{54^{1/3}} - \frac{2^{1/3}S2}{3Sh}\right) - \frac{1}{2}\left(\frac{Sh}{54^{1/3}} + \frac{2^{1/3}S2}{3Sh}\right) \quad (11.2)$$

$$\omega_c = \frac{\Delta_s}{3} - \frac{i}{2}\sqrt{3}\left(\frac{Sh}{54^{1/3}} - \frac{2^{1/3}S2}{3Sh}\right) - \frac{1}{2}\left(\frac{Sh}{54^{1/3}} + \frac{2^{1/3}S2}{3Sh}\right) \quad (11.3)$$

and the eigenvectors can be expressed as

$$\Phi_i = \frac{1}{N_i}\left(\frac{\Omega_p}{\Omega_s}\left(-\frac{\Delta_s}{\omega_i} + 1\right)|1\rangle + \frac{-\Delta_s + \omega_i}{\Omega_s}|2\rangle + |3\rangle\right)e^{-i\Gamma_i(t)} \quad (12.1)$$

$$\Gamma_i(t) = \int_{-\infty}^t \omega_i dt', \quad i = a, b, c \quad (12.2)$$

where N_i is a normalization factor. The general solution is expanded by the linear combination of Φ_i

$$\Psi = \sum_i \alpha_i \Phi_i, \quad i = a, b, c \quad (13)$$

Using the initial condition $\Psi|_{t \rightarrow -\infty} \rightarrow |1\rangle$ one obtains

$$\alpha_i = \frac{\Omega_p}{\Omega_s}\left(\frac{-\Delta_s}{\omega_i} + 1\right), \quad i = a, b, c \quad (14)$$

The general solution expanded by linear combination of $|1\rangle$, $|2\rangle$, and $|3\rangle$ is expressed as

$$\Psi = \beta_1|1\rangle + \beta_2|2\rangle + \beta_3|3\rangle \quad (15)$$

where

$$\beta_1 = \sum_{i=a,b,c} \alpha_i^2 \frac{e^{-i\Gamma_i(t)}}{N_i} \quad (16.1)$$

$$\beta_2 = \sum_{i=a,b,c} \alpha_i \left(\frac{-\Delta_s + \omega_i}{\Omega_s}\right) \frac{e^{-i\Gamma_i(t)}}{N_i} \quad (16.2)$$

$$\beta_3 = \sum_{i=a,b,c} \alpha_i \frac{e^{-i\Gamma_i(t)}}{N_i} \quad (16.3)$$

Then the element of the density matrix can be expressed as

$$\rho_{11} = \beta_1 \cdot \beta_1 \quad (17.1)$$

$$\rho_{22} = \beta_2 \cdot \beta_2 \quad (17.2)$$

$$\rho_{33} = \beta_3 \cdot \beta_3 \quad (17.3)$$

$$\rho_{23} = \beta_2 \cdot \beta_3 \quad (17.4)$$

The above density matrix elements could be probed by various experimental schemes.

B. Comparison with the Experiment. The signal registered under the scheme of polarization spectroscopy is the last term of eq 1. In terms of density matrix form the signal can be expressed as

$$I \propto \int_{-\infty}^{+\infty} ((\rho_{22} e^{-\gamma t} - \rho_{33})\rho_{23}\Omega_s)^2 dt \quad (18)$$

where γ represents the total relaxation of ρ_{22} . State $|3\rangle$ in this case is $J = 32$, $(3 \ 18 \ 0)$, $X^1\Sigma_g^+$ state which possesses a long lifetime. Therefore, the relaxation of ρ_{33} can be neglected. The polarization $(\Delta\alpha)^2$ is represented by $(\rho_{22}e^{-\gamma t} - \rho_{33})^2$. The term $(\rho_{23}\Omega_s)^2$ represents stimulated emission registered in the scheme of polarization spectroscopy. The relaxation and stimulated emission in the above equations are phenomenologically treated to resemble the intensity of the stimulated emission in a rate equation approach.

Each of the applied laser field is represented by a gaussian pulse

$$\Omega_p = C_p e^{-t^2/T^2} \quad (19.1)$$

$$\Omega_s = C_s e^{-(t-C_s)^2/T^2} \quad (19.2)$$

C_p and C_s are the magnitudes of the Rabi frequency for the pump and s-active transitions, respectively. C_i is the delay time and is negative when the s-active pulse precedes the pump pulse. The half-width at half-maximum of the pulse duration, T , was measured to be 12.5 ns with a 2.5 ns fluctuation. The two pulses do not have phase relationship because they were generated by two separate lasers, and the spatially varying laser intensity was ignored.¹⁸ One could experimentally pretune the frequency of the s-active photon pulse to the exact resonance but could not assume that detuning is zero. One has to take the detuning caused by the splitting into account. This non-zero detuning is associated with spectral line width and power broadening. The detuning Δ_s , therefore, is expressed as

$$\Delta_s = [C_g + S_p(x)]e^{-(t-C_s)^2/T^2} e^{-x^2/\delta^2} \quad (20)$$

Δ_s processes both time domain and frequency domain profiles and varies with the s-active photon pulse intensity. The magnitude of Δ_s consists of two terms. C_g represents the pre-detuning, while $S_p(x)$ represents detuning caused by spectral line width and power broadening. $S_p(x)$ is assumed to be linear function with line width. The term $e^{-(t-C_s)^2/T^2}$ represents the profile in time domain. The term e^{-x^2/δ^2} represents the profile in frequency domain. The laser line width δ is 0.2 cm^{-1} .

Figure 5 shows the time delay scans recorded under various experimental conditions. The points are the experimental observations, while solid curves are simulations based on eq 18. The signal profiles are sensitive to the experimental factors

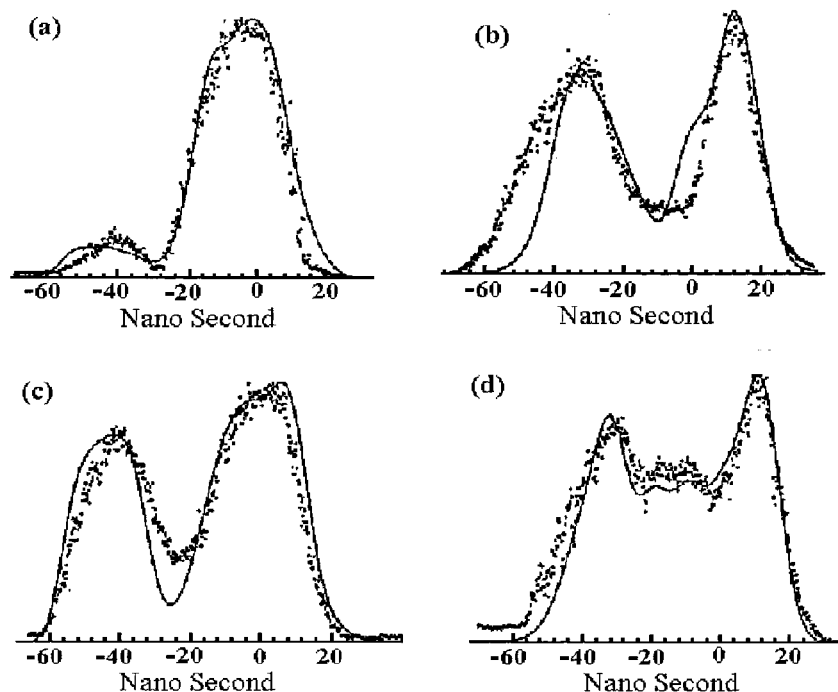


Figure 5. The delay time scans. The experimental factors for each scan are listed in Table 1. Points are experimental observations, while the curve is the simulation results from the dressed state approach. Scans 5a and 5b show a comparison of applied weak stimulating laser intensity with strong one. Scans 5a and 5c comparatively illustrate that the profile of delay time scan varies not only with laser intensity but also with detuning, relaxation, and line width. Scan 5d shows a profile with four-peaked feature which results from two incoherent pulses interacting.

TABLE 1: Values of Experimental Factors and Fitting Parameters Which Were Used in Figure 5

	5a	5b	5c	5d
I_p (mJ)	3.8	3.7	5.8	1.0
I_s (mJ)	0.38	3.2	0.48	13
pre-detuning ($10^9/s$)	no	6.16	yes	yes
C_p (10^5)	0.25	0.72	0.22	0.72
C_s (10^8)	0.12	4.9	0.3	2.5
C_g (10^8)	3.0	0.04	4.5	0.04
S_p	1.0	1.0	3.0	1.0
γ	0.5	2.0	0.41	2.5

such as laser intensity, detuning and pressure. The simulation has five fitting parameters C_p , C_s , C_g , S_p , and γ . The value of the experimental factor and the resulting fitting parameters are listed in Table 1. The guessing value of each parameter could be estimated from the associated experimental factor except C_s . The estimated value of C_p was deduced from the absorption cross section of the pump transition and intensity of the pump photon pulse. The absorption cross section at ω_p was measured to be $\sigma_p = 1.71 \times 10^{-19} \text{ cm}^2$ which corresponds to an oscillator strength of 6.5×10^{-7} . To estimate the photon intensity the beam waist was measured to be $0.5 \sim 1.0 \times 10^{-2} \text{ cm}$. The above values yield Ω_p of $10^4 \sim 10^5/s$ which is consistent with the fitting value of C_p listed in Table 1. Although the value of C_s could be qualitatively estimated from the plot of splitting vs intensity of the s-active laser under the assumption that the splitting is proportional to $(\Omega_p^2 + \Omega_s^2)^{1/2}$,¹⁷ the estimation was not quantitatively acceptable. Besides, the induced transition dipole moment μ_s is not easily measured directly. Therefore, C_s was treated as a free fitting parameter in the simulation. The best fitted value of C_s is on the order of 10^9 . Hence, μ_s/μ_p is on the order of at least 10^4 . The studies of the lifetime (on the order of μs)¹⁹ and the fluorescence²⁰ of $|2\rangle$ state excludes large Frank–Condon overlap from the possible reason for such a large value. The strong emission may be caused by collective emission effect.²⁰ Thus, the physical meaning of μ_s is ambiguous and is rather to be regarded as an effective transition dipole moment. Both the values of C_g and S_p are closely related to the splitting.

The splitting, which ranged from 0.1 to 0.5 cm^{-1} , results in the value of C_g being on the order of $10^9 \sim 10^{10} \text{ (s}^{-1}\text{)}$ and the value of S_p one to three times larger than the laser line width. Among these parameters the relaxation γ is the most sensitive. It represents both radiative decay and nonradiative decay. Because of the latter, the value of γ varied with the pressure in the cell. The pressure could not be maintained constant, instead it gradually increased during the experiment. The pressure increase was caused by degas from the cell wall and dissociation of CS_2 . The latter was significant under the laser intensity applied in the experiment. This drawback was difficult to be controlled by the experiment. Additional drawback caused by the CS_2 pressure is that intensity of the lasers was attenuated by the burns on the window of the cell. This is commonly encountered in a high-power laser application, especially in a static cell case. Since the degree of burn was varying, neither the intensity of the pump photon pulse nor the s-active photon pulse could be considered constant values during the experiment. But the simulation, without compensating the above drawbacks, reasonably resembles the experimental result at least qualitatively. For instance, the value of C_s is smaller in Figure 5a than that in Figure 5b, which is consistent with the photon intensities applied to yield the two figures. The intensity effect is not always apparent, as is illustrated from a comparison of parts a, b, and c of Figure 5, when the characteristics of spectra were dominated by relaxation or detuning. Figure 5d shows a spectrum with a four-peaked feature. It was surprising and difficult to understand how it could result from two incoherent pulses interacting. The intuitive answer is that this feature might be an “interference pattern” provided that the pulse relationship was somehow defined by the process of stimulated emission. On the other hand, such a multi-peaked feature was successfully simulated by using the dressed state approach in which no defined phase relationship between two lasers was needed. The term “interference” in dressed state approach might find its analog to the cross terms of combined wave function as expressed in eq 15. However, influenced by detuning and relaxation it is implicit to link the two together during the

evolution of the dressed state wave function. The successful simulations in Figure 5 demonstrate that when CS₂ molecules interact with photon intensity of several millijoules, the system, instead of being treated as pure molecular states interacting with photon fields, is better described by the dressed state approach.

IV. Conclusion

In the fashion of “counterintuitive sequence”, stimulated emission has been observed in the scheme of polarization spectroscopy. Viewing from the dressed state approach, the term “counterintuitive sequence” can be understood as a consequence of transient state emission. The eigenfunction for the dressed state was derived by explicitly solving the Hamiltonian that describes a three-level system subjected to two pulsed laser fields with a detuning from the s-active photon resonance. Values of the parameters in the simulation compare reasonably well with experimental quantities. The complicated profile in the time delay scans can not result from two-pulse interaction, rather it reflects the evolution of the transient state under the influence of detuning and relaxation. The analysis showed that the efficiency of population transfer could be manipulated not only by the sequence of interacting fields but also be the characteristics of the laser fields.

In conclusion, we shall note that an unexpectedly large Rabi frequency for the s-active photon in the simulation remains unexplained. So far, we would only suspect that the emission may not follow eq 18 exactly. The equation may need to be modified to take the mechanism of collective emission into account²⁰ and to be a subject of the future study.

Acknowledgment. H.T. Liou thanks Dr. A. kung and Dr. K. Liu for their valuable discussion. This research is supported,

in part, by National Science Council, R.O.C., under grant no. NSC 85-2113-M-001-022.

References and Notes

- (1) Oreg, J.; Hioe, F. T.; Eberly, J. H. *Phys. Rev. A* **1984**, *29*, 690.
- (2) Gaubatz, U.; Rudecki, P.; Schiemann, S.; Bergmann, K. *J. Chem. Phys.* **1990**, *92*, 5363.
- (3) Schiemann, S.; Kuhn, A.; Steuerwald, S.; Bergmann, K. *Phys. Rev. Lett.* **1993**, *71*, 3637.
- (4) Gaubatz, U.; Rudecki, P.; Becker, M.; Schiemann, S.; Külz, M.; Bergmann, K. *Chem. Phys. Lett.* **1988**, *149*, 463.
- (5) Halfmann, T.; Bergmann, K. *J. Chem. Phys.* **1996**, *104*, 7068.
- (6) Khidekel, V.; Fain, B.; Liou, H. T.; Lin, S. H. *Chem. Phys. Lett.* **1995**, *234*, 39.
- (7) Wells, J. S.; Schneider, M.; Maki, A. G. *J. Mol. Spectrosc.* **1988**, *132*, 422.
- (8) Merer, A. J.; Morris, S. A. *J. Mol. Spectrosc.* **1988**, *127*, 425.
- (9) Liou, H. T.; Dan, P.; Yang, H.; Yuh, J. Y. *Chem. Phys. Lett.* **1991**, *176*, 109.
- (10) Tees, R. E.; Kowalski, F. W.; Hill, W. T.; Carlston, N.; Hänsch, T. W. In SPIE, Vol. 113, *Laser Spectroscopy*, San Diego, CA, 1977; p 80.
- (11) Demtröder, W. *Laser Spectroscopy*, Springer Series in Chemical Physics Vol. V; New York, 1982; p 511.
- (12) Gray, H. R.; Stroud, C. R., Jr. *Opt. Commun.* **1978**, *25*, 359.
- (13) Townes, C. H.; Schawlow, A. L. *Microwave Spectroscopy*; Dover: 1975; p 279.
- (14) Martin, J.; Shore, B. W.; Bergmann, K. *Phys. Rev. A* **1996**, *54*, 1556.
- (15) Neuhauser, R.; Neusser, H. J. *J. Chem. Phys.* **1995**, *103*, 5362.
- (16) Linskens, A. F.; Dam, N.; Reuss, J.; Sartakov, B. *J. Chem. Phys.* **1994**, *101*, 9384.
- (17) Gray, H. R.; Whitley, R. M.; Stroud, C. R., Jr. **1978**, *3*, 218.
- (18) Neuhauser, R.; Sussmann, R.; Neusser, H. J. *Phys. Rev. Lett.* **1995**, *74*, 3141.
- (19) Liou, H. T.; Yan, H.; Wang, N. C.; Joy, R. *Chem. Phys. Lett.* **1991**, *178*, 80.
- (20) Liou, H. T.; Yang, H.; Dan, P. *Appl. Phys. B* **1992**, *54*, 221.